C–H Bond Activation by Cationic Iridium(III) NHC Complexes: A Combined Experimental and Computational Study

ARTICLE *in* ORGANOMETALLICS · FEBRUARY 2012

Impact Factor: 4.13 · DOI: 10.1021/om2012166

5 AUTHORS, INCLUDING:

Robert Robinson Jr
University of Tasmania
8 PUBLICATIONS **26** CITATIONS
SEE PROFILE

Karen Goldberg
University of Washington Seattle
118 PUBLICATIONS **5,027** CITATIONS
SEE PROFILE

Werner Kaminsky
University of Washington Seattle
280 PUBLICATIONS **3,800** CITATIONS
SEE PROFILE

ORGANOMETALLICS

Article

pubs.acs.org/Organometallics

C–H Bond Activation by Cationic Iridium(III) NHC Complexes: A Combined Experimental and Computational Study

Joseph M. Meredith, Robert Robinson, Jr., Karen I. Goldberg, Werner Kaminsky, and D. Michael Heinekey*

Department of Chemistry, University of Washington, Box 351700, Seattle, Washington 98195-1700

Supporting Information

ABSTRACT: The cationic complexes $[Cp^*Ir(NHC)Me(solv)]^+[MeB(C_6F_5)_3]^-$ were prepared and studied as models for methane oxy-functionalization catalysts ($Cp^* = \eta^5\text{-}C_5Me_5$; NHC = 1,3,4,5-tetramethylimidazol-2-ylidene (MeI^{Me}, **3a**), 1,3-dimethylimidazol-2-ylidene (I^{Me}, **3b**), 1,3-dimethylbenzimidazol-2-ylidene (BI^{Me}, **3c**); solv = solvent or open site). These complexes were targeted on the basis of the C–H bond activation reactions of the previously reported complexes $[Cp^*Ir(PMe_3)R]^+$ (R = Me, H) and the general robustness of Ir–NHC complexes under oxidizing conditions. The syntheses of the new iridium(III) complexes $Cp^*Ir(NHC)Me_2$ are described (NHC = MeI^{Me} (**4a**), I^{Me} (**4b**), BI^{Me} (**4c**)). When **4a–c** were allowed to react with $B(C_6F_5)_3$ in CH_2Cl_2, the methyl abstraction products $[Cp^*Ir(NHC)Me(solv)]^+[MeB(C_6F_5)_3]^-$ (**3a–c**) were produced. Complexes **3a–c** reacted with arenes to form the aryl complexes $[Cp^*Ir(NHC)Ar(solv)]^+[MeB(C_6F_5)_3]^-$ and methane (Ar = C_6H_5 (**7**), C_6H_4F (**8**)). Complexes **3a–c** reacted very slowly with alkanes; the slow reaction rate is attributed to steric congestion due to the NHC ligand. DFT calculations support this hypothesis: the barriers to C–H activation are in qualitative agreement with the empirical reaction rates, and the C–H activation transition state structures show significant steric crowding. Several of these complexes have been analyzed by X-ray diffraction.

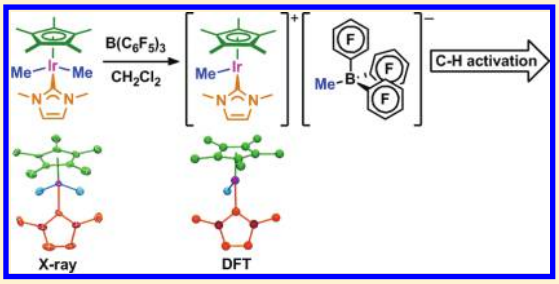

INTRODUCTION

Despite years of effort, a practical process for the direct catalytic oxidation of methane to methanol remains elusive. Although an industrially applicable process will likely require a heterogeneous catalyst, much work has been directed at homogeneous systems, with the hope that they will teach us enough to create effective heterogeneous catalysts. Most of this work has been limited to soluble complexes of platinum(II),[1] while relatively little effort has been directed toward exploring iridium complexes as catalysts for methane oxidation. Recently, Periana and co-workers disclosed a system for the conversion of methane to methyl trifluoroacetate promoted by an iridium(III) pincer complex (**1**; Chart 1).[2] Unfortunately, catalysis by **1** is only observed with the oxidants MIO_4 and MIO_3 (M = Na, K) and this catalytic system is less efficient than those reported previously.[3] A system capable of selectively oxidizing methane using O_2 as the oxidant is more desirable.

Chart 1

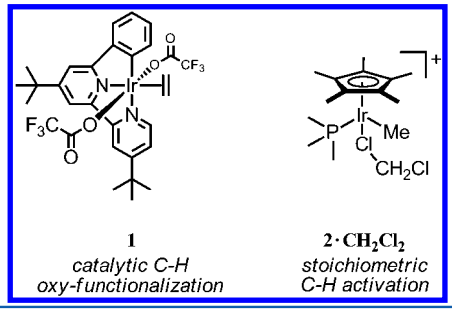

Methane functionalization with O_2 requires a catalyst that is capable of activating sp^3-hybridized C–H bonds *and* is compatible with reoxidation by O_2. Bergman and co-workers showed that the complex $[Cp^*Ir(PMe_3)Me(CH_2Cl_2)]^+$ ($Cp^* = \eta^5\text{-}C_5Me_5$, $\mathbf{2}\cdot CH_2Cl_2$) reacted with sp^3-hybridized C–H bonds of alkanes, including methane, under mild conditions.[4] This system was not employed for methane oxy-functionalization because the PMe_3 ligand is readily oxidized to $O{=}PMe_3$. Substitution of the PMe_3 ligand with an N-heterocyclic carbene (NHC) ligand would give the complex $[Cp^*Ir(NHC)Me(solv)]^+$ (solv = solvent or open site; **3**), which would not be susceptible to the same type of decomposition as $\mathbf{2}\cdot CH_2Cl_2$ (Chart 2). We set out to synthesize **3** and determine its ability to activate C–H bonds. We hypothesized that **3** would retain the C–H bond activation chemistry of $\mathbf{2}\cdot CH_2Cl_2$ while possessing greater stability under oxidizing conditions.

Complexes of NHC ligands with bulky N substituents often undergo cyclometalation reactions.[5] To avoid formation of cyclometalated products, we focused on NHC ligands with N–methyl substituents. The NHC ligands MeI^{Me}, I^{Me}, and BI^{Me} fit this criterion and represent a modest range of electron-donating character, as shown in Chart 3 (MeI^{Me} = 1,3,4,5-tetramethylimidazol-2-ylidene (**a**); I^{Me} = 1,3-dimethylimidazol-2-ylidene (**b**);

Received: December 7, 2011
Published: February 7, 2012

   dx.doi.org/10.1021/om2012166 | Organometallics 2012, 31, 1879–1887

Chart 2

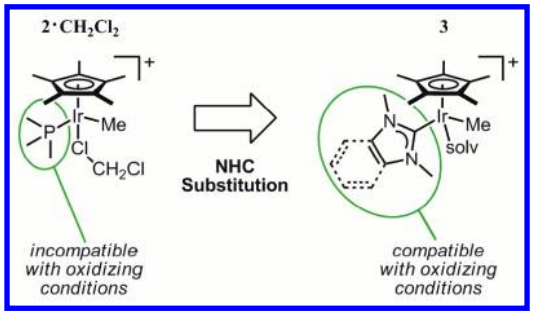

Chart 3. NHC Ligands Used and Comparison of Their Predicted[6] Tolman Electronic Parameters (TEPs)[a]

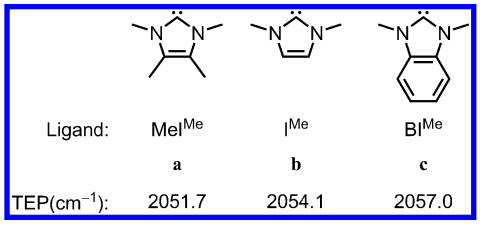

[a]PMe_3 has TEP = 2064.1 cm^{-1}.

BI^{Me} = 1,3-benzimidazol-2-ylidene (**c**)). The predicted Tolman electronic parameters (TEPs) of NHC ligands **a**–**c** suggest that the iridium atoms in complexes **3a**–**c** will be more electron-rich than those of **2**·CH_2Cl_2.[6]

RESULTS AND DISCUSSION

The complexes Cp*Ir(NHC)Me_2 (**4a**–**c**) were synthesized from the corresponding Cp*Ir(NHC)Cl_2 species[7] via Grignard alkylation in good yields (60–74%). Complexes **4a**–**c** are air-stable yellow crystalline solids, which were characterized by ^1H and ^{13}C NMR spectroscopy. The Ir–Me groups resonate between −0.05 and 0.08 ppm in the ^1H NMR spectra and between −19.94 and −21.04 ppm in the ^{13}C NMR spectra (CD_2Cl_2). The $C_{carbene}$ signals of **4a**–**c** were observed in the $^{13}C\{^1H\}$ NMR spectra at 163.91, 165.96, and 181.88 ppm, respectively. Complexes **4a** and **4b** were further characterized by single-crystal X-ray diffraction. The ORTEP diagram of **4b** is displayed in Figure 1.[8] A three-legged piano-stool geometry was

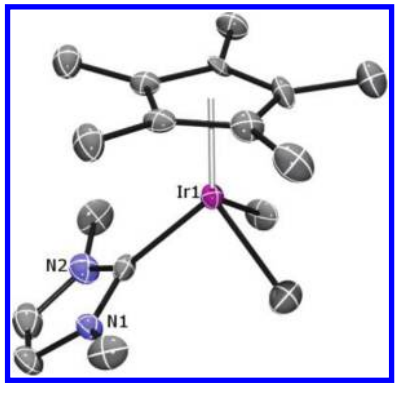

Figure 1. ORTEP of Cp*Ir(I^{Me})Me_2 (**4b**). Hydrogen atoms have been omitted for clarity. Ellipsoids are displayed at the 50% probability level.

observed, with the Cp* ligands acting as the capping groups. The Ir–$C_{carbene}$ bond lengths are very similar: 2.004 Å (±0.007 Å, **4a**) and 1.997 Å (±0.007 Å, **4b**).

The reagent $B(C_6F_5)_3$ was used to convert dimethyl complexes **4a**–**c** to cationic monomethyl complexes [Cp*Ir(NHC)Me(solv)]$^+$[$MeB(C_6F_5)_3$]$^-$ (**3a**–**c**) in quantitative yield (by ^1H NMR spectroscopy, Scheme 1). Complexes **3a**–**c** are

Scheme 1. Reaction between Cp*Ir(I^{Me})Me_2 (4b) and $B(C_6F_5)_3$

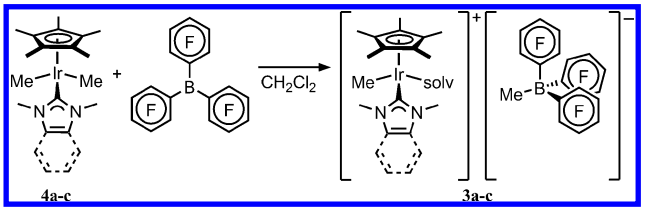

dark red-brown[9] and are highly air-sensitive.[10] Attempts to crystallize **3a**–**c** were not successful.

The ^1H NMR spectra (CD_2Cl_2) of **3a**–**c** exhibit signals for the Ir–Me and B–Me moieties at 2.36–2.41 and 0.46 ppm, respectively (Figure 2). The Ir–Me signals of **3a**–**c** are shifted

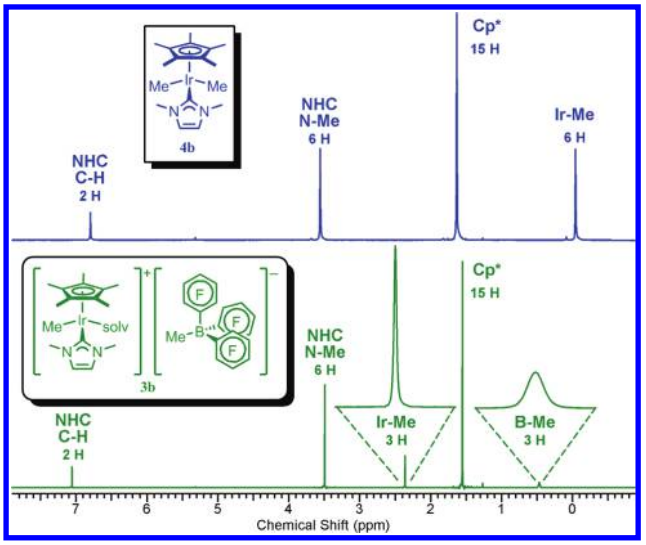

Figure 2. ^1H NMR spectra (500 MHz, CD_2Cl_2, 25 °C): (top) Cp*Ir(I^{Me})Me_2 (**4b**); (bottom) [Cp*Ir(I^{Me})Me]$^+$[$MeB(C_6F_5)_3$]$^-$ (**3b**).

downfield from the Ir–Me signals of **4a**–**c** by nearly 2.5 ppm, consistent with the change in charge upon Me^- abstraction. The Ir–Me signals for **3a**–**c** exhibit normal C–H coupling constants for sp^3-hybridized C–H bonds (126 Hz),[11] excluding the possibility of an α-agostic interaction between Ir and the methyl ligand.[12] The line widths of the Ir–Me signals are the same as the signals for the Cp* and NHC ligands (1 Hz). The B–Me signal is broader than the other signals of **3a**–**c** (10 Hz). The broadness of the B–Me signal is attributed to rapid relaxation of these protons caused by the quadrupolar boron nucleus.

The [$MeB(C_6F_5)_3$]$^-$ counteranion is generally noncoordinating, but there are examples of [$MeB(C_6F_5)_3$]$^-$ acting as a ligand.[13] However, the [$MeB(C_6F_5)_3$]$^-$ counteranion does not act as a ligand in **3a**–**c**: the ^1H, ^{11}B, $^{13}C\{^1H\}$, and ^{19}F NMR spectra of the counteranions in **3a**–**c** match the reported values for free [$MeB(C_6F_5)_3$]$^-$.[14] Additionally, the NMR spectra of the counteranions in **3a**–**c** are identical with those of the counteranion in [n-Bu_4N]$^+$[$MeB(C_6F_5)_3$]$^-$ and the coordinatively saturated complex [Cp*Ir(I^{Me})Me(CO)]$^+$[$MeB(C_6F_5)_3$]$^-$ (**5b**).

dx.doi.org/10.1021/om2012166 | Organometallics 2012, 31, 1879–1887

Complex **3b** reacts with CO to form the coordinatively saturated complex **5b** in high yield. The structure of **5b** was confirmed by ^{1}H NMR, ^{13}C NMR, and infrared spectroscopies. The Cp* and Ir−Me ^{1}H NMR signals were observed as sharp singlets. However, the NHC C−H and N−Me signals are broad at room temperature (Figure 3). Upon cooling, these

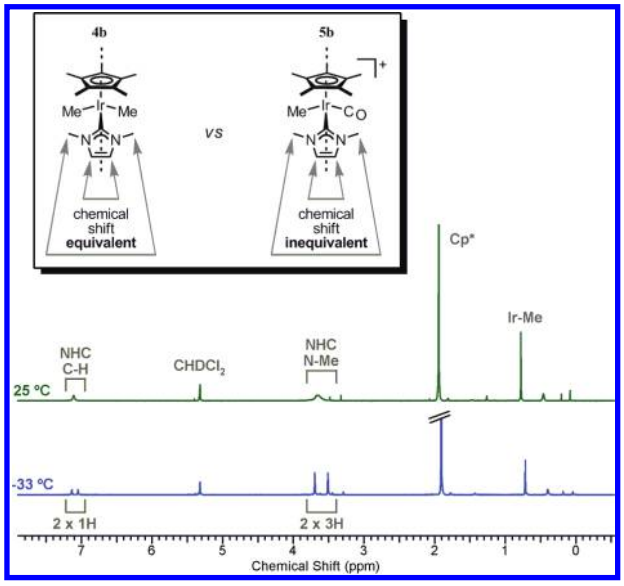

Figure 3. ^{1}H NMR spectra (500 MHz, CD_2Cl_2) of **5b** at 25 °C (bottom) and −33 °C (top). The chemical environments for the NHC C−H and N−Me groups of $Cp^*Ir(I^{Me})Me_2$ (**4b**) and $[Cp^*Ir(I^{Me})Me(CO)]^+$ (**5b**) are compared in the inset.

resonances decoalesced into two pairs of sharp signals, which are attributed to the two sets of NHC C−H and N−Me groups (one proximal and one distal to the CO ligand; Figure 3, inset). The infrared spectrum of **5b** exhibits one carbonyl band with a stretching frequency appropriate for a cationic Ir^{III} monocarbonyl (2024 cm^{-1}).[15] The complex $[Cp^*Ir(PMe_3)Me(CO)]^+$ shows a higher value for ν_{CO} (2035 cm^{-1}),[16] consistent with the assertion that **3b** is more electron-rich than its PMe_3-ligated counterpart.

The CH_2Cl_2 ligand of **2**·CH_2Cl_2 is quite labile; therefore, it is reasonable to assume that CH_2Cl_2 would bind weakly, if at all, in **3a−c**. The complexes **3a−c** were analyzed by low-temperature ^{1}H NMR spectroscopy to determine whether they were best described as the 16 e^- coordinatively unsaturated complexes $[Cp^*Ir(NHC)Me]^+$ or as the 18 e^- solvento species $[Cp^*Ir(NHC)Me(CD_2Cl_2)]^+$. The latter structure has C_1 symmetry and would result in a ^{1}H NMR spectrum similar to the observed spectrum for **5b** (Figure 3). The 16 e^- structure would likely have C_s symmetry[17] and would result in a simplified ^{1}H NMR spectrum, similar to the ^{1}H NMR spectra of **4a−c** and the spectra of **3a−c** acquired at 25 °C. The ^{1}H NMR spectra of **3a−c** were recorded between 25 and −70 °C. The ^{1}H resonances of the NHC ligand varied slightly with temperature, but the line shape and number of signals did not. These data are consistent with the 16 e^- structure. However, the same NMR spectra would result if **3a−c** adopted the solvent-bound 18 e^- structure *and* the solvent ligand exchanged rapidly (on the NMR time scale) with bulk solvent. The low-temperature NMR spectral data do not refute either structure, but the data do suggest that if CH_2Cl_2 acts as a ligand in **3a−c**, it is highly labile.

In the presence of traces of moisture, dichloromethane solutions of **3a−c** decompose to the dicationic bimetallic complexes $[\{Cp^*Ir(NHC)(\mu\text{-}Cl)\}_2]^{2+}[(MeB(C_6F_5)_3)^-]_2$ (**6a−c**), which have limited solubility in dichloromethane (Scheme 2).

Scheme 2. Conversion of $[Cp^*Ir(NHC)Me(solv)]^+$ (3a−c) to $[\{Cp^*Ir(NHC)(\mu\text{-}Cl)\}_2]^{2+}$ (6a−c)

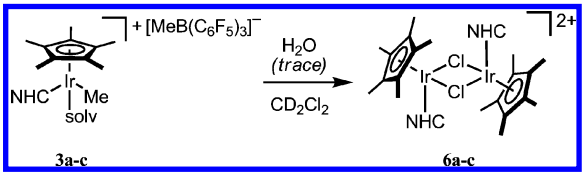

Complexes **6a−c** were typically isolated in low yields (ca. 10%, crystals). The synthesis of complex **6a** with $[OTf]^-$ counteranions was reported recently by Ison and co-workers (OTf = trifluoromethanesulfonate).[18] Ison found that treatment of $Cp^*Ir(MeI^{Me})Cl_2$ with $Ag[OTf]^-$ in dichloromethane produced **6a**·2OTf^- in good yield. Independent syntheses of **6a−c** (with $[MeB(C_6F_5)_3]^-$ counteranions) by treatment of dichloromethane solutions of **3a−c** with excess water were not successful. After monitoring these reactions by NMR, we suspect that, in the presence of excess water, the aquo complexes $[Cp^*Ir(NHC)Me(OH_2)]^+$ are formed instead of **6a−c.** The structure of **6b** was determined by X-ray diffraction. An ORTEP diagram of **6b** is shown in Figure 4. Both Ir centers

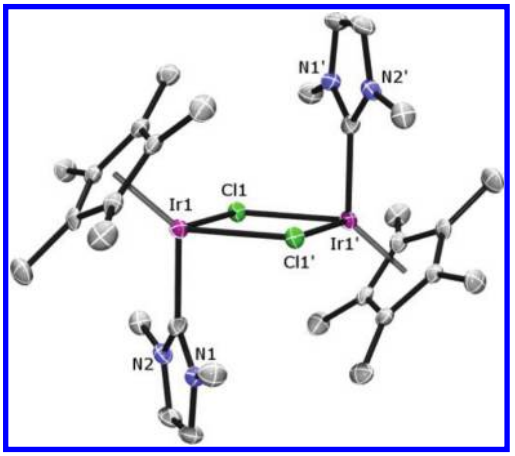

Figure 4. ORTEP of $[\{Cp^*Ir(I^{Me})(\mu\text{-}Cl)\}_2]^{2+}[(MeB(C_6F_5)_3)^-]_2$ (**6b**). Hydrogen atoms and both $[MeB(C_6F_5)_3]^-$ counteranions have been omitted for clarity. Ellipsoids are depicted at the 50% probability level.

adopt three-legged piano-stool geometries, with the Cp* ligands as the capping groups. Despite the different NHC ligands and counteranions, the structure of **6b** is nearly identical with the structure reported by Ison and co-workers.[18]

Similar results were reported by Gladysz and co-workers, who found that $[(C_5R_5)Re(NO)(PPh_3)(CH_2Cl_2)]^+$ decomposed to dimeric products with bridging chloride ligands (R = H, Me).[19] It was shown that the Cl atom in their bimetallic products originated in the CH_2Cl_2 solvent.[20] In the case of **6b**, the only source of Cl atoms is the CH_2Cl_2 solvent.

Bergman and co-workers observed the decomposition of **2**·CH_2Cl_2 in dichloromethane solution above 0 °C. We expected complexes **3a−c** to exhibit similar thermal instability. However, under an inert atmosphere in the absence of light,[21] **3a−c** are stable in dry dichloromethane solution for extended

dx.doi.org/10.1021/om2012166 | *Organometallics* 2012, 31, 1879−1887

periods at room temperature. The mechanism of the interesting chloride abstraction reaction to form **6a–c** remains obscure, but the participation of adventitious water is implicated by the failure to observe this reaction in carefully dried solvent.

C–H Activation Studies. Bergman and co-workers found that **2**·CH_2Cl_2 activated the C–H bonds of alkanes and arenes at or below room temperature, in minutes to hours.[4,22] For example, the reaction between **2**·CH_2Cl_2 and benzene reportedly results in "immediate effervescence, due to methane loss."[4] We were surprised to find that **3a–c** were much less reactive toward C–H bonds. For example, the reaction between **3a** or **3b** and benzene requires hours to go to completion, even in the presence of a large excess of benzene; the reaction with C_6H_5F is slower, reaching full conversion after *ca.* 2.5 days in neat fluorobenzene. In these reactions methane was produced and

Scheme 3. Reaction between [Cp*Ir(NHC)Me(solv)]$^+$ and Arenes (Benzene and Fluorobenzene)

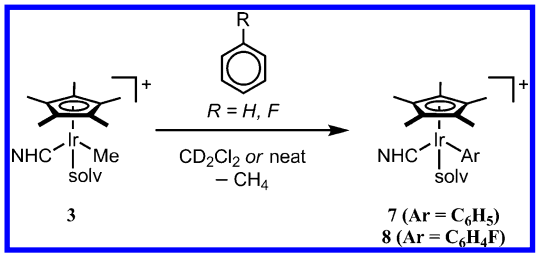

the iridium aryl products [Cp*Ir(NHC)Ar(solv)]$^+$[$MeB(C_6F_5)_3$]$^-$ (Ar = C_6H_5, **7a,b**; Ar = C_6H_4F, **8a**) were observed by NMR spectroscopy (Scheme 3). When **3a** was allowed to react with C_6D_5F, CH_3D was observed as a product. Complex **8a** was formed as a mixture of ortho, meta, and para isomers.[23]

Interestingly, alkanes are activated so slowly by **3a–c** that a reaction is only observed in the presence of large excesses of alkane after extended reaction periods (alkane = pentane, cyclohexane, isobutane). For example, after 28 days, a mixture of **3c** and cyclohexane showed 16% conversion to a new species that was tentatively assigned as the product of C–H activation followed by methane release and β-hydride elimination: [Cp*Ir(BI^{Me})(H)(cyclohexene)]$^+$. Heating accelerated C–H activation but caused significant decomposition. We hypothesized that the low steric profile of methane may make it more amenable to activation by **3a–c**. To investigate the possibility of a reaction with CH_4, we prepared the ^{2}H-labeled complex [Cp*Ir(BI^{Me})(CD_3)(solv)]$^+$[$(CD_3)B(C_6F_5)_3$]$^-$ (**3c-d_6**). A dichloromethane-d_2 solution of **3c-d_6** was exposed to CH_4 (3 atm, 99.999% pure) and observed by NMR spectroscopy. No signals for protiated Ir–Me groups were observed, even after 5 weeks at room temperature. Presumably, the reaction with methane is slower than reactions with other alkanes because the concentration of methane is lower.

An explanation for the slow C–H activation reactions of **3a–c** may be gained by examining the reaction mechanism. The mechanism of C–H activation by **2**·CH_2Cl_2 has been the subject of considerable study. The two potentially viable mechanisms that have received the most attention are oxidative addition/reductive elimination (OA/RE) and σ-bond metathesis (SBM).[24] The OA/RE and SBM mechanisms are illustrated in Scheme 4. Both mechanisms begin with the same step: CH_2Cl_2 dissociation from **2**·CH_2Cl_2 leads to a reactive 16 e$^-$ species (**2**), which could potentially activate C–H bonds by OA/RE or SBM mechanisms. The product of OA is a seven-coordinate Ir^V complex (**9**). Complex **9** can reductively eliminate substrate R–H (nonproductive) or CH_4 (productive), to afford a coordinatively unsaturated product. If the R group contains β-H atoms (e.g., R = *n*-alkyl), products of the form [Cp*Ir(PMe_3)(olefin)(H)]$^+$ are isolated. If R does not contain β-hydrogen atoms (e.g., R = Ph), then [Cp*Ir(PMe_3)(R)(CH_2Cl_2)]$^+$ products are obtained instead. In the SBM mechanism, complex **2** reacts with substrate (R–H) via a four-centered transition state (**10**) that contains an Ir^{III} center.

The intermediacy of **9** has been regarded with some skepticism,[25] as complexes of iridium in the +5 oxidation state are rare.[26] Following some of the computational results[24] which implicated **9**, relevant complexes of Ir^V containing the Cp*Ir(PMe_3) unit were reported.[17,22,27] Although complex **9** has not been isolated, the discovery of additional Ir^V species has lent credence to the idea of an Ir^{III}/Ir^V redox couple in C–H activation reactions.[28] SBM reactivity is a hallmark of d^0 early-transition-metal complexes, which are electron-deficient.[29] The SBM mechanism seems less likely for a late-transition-metal complex with electron-donating ligands, such as **2**·CH_2Cl_2.

Why are the NHC–ligated complexes less reactive toward C–H bonds? The electron-donating NHC ligands should *electronically* stabilize a seven-coordinate Ir^V intermediate, relative to [Cp*Ir(PMe_3)Me]$^+$. However, as more sterically demanding ligands than PMe_3, the NHCs may *sterically* disfavor formation of crowded seven-coordinate Ir^V species. Therefore, the difference in C–H activation rates between the NHC and

Scheme 4. Possible Mechanisms for C–H Activation by [Cp*Ir(PMe_3)Me(CH_2Cl_2)]$^+$ (2·CH_2Cl_2)

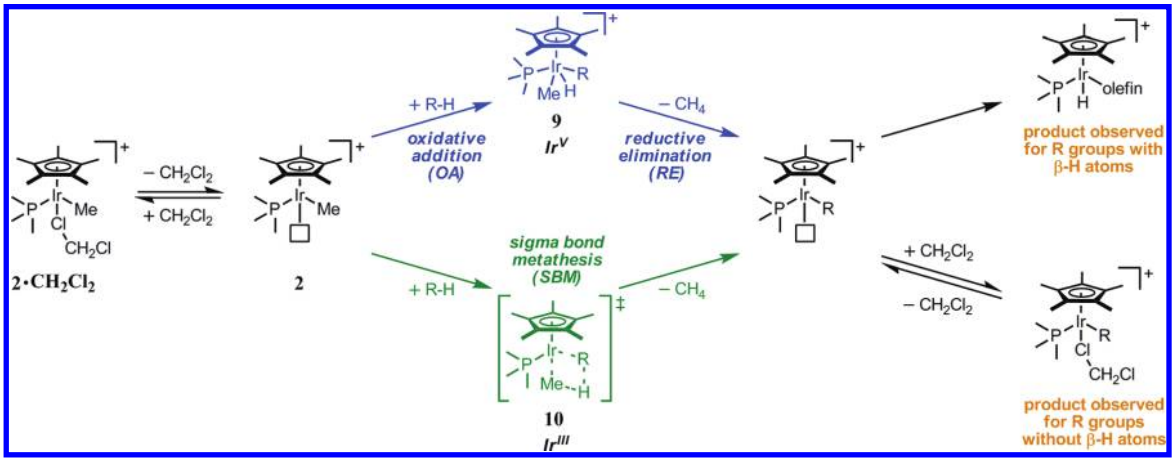

dx.doi.org/10.1021/om2012166 | *Organometallics* 2012, 31, 1879–1887

PMe_3 complexes may be attributed to a steric effect. To evaluate this hypothesis, we turned to density functional theory (DFT) calculations.

DFT calculations (B3LYP) were explored to determine the lowest-energy mechanism for C−H activation by complexes **2** and **3b** (Chart 4). Calculations were carried out for reactions between each complex and methane or benzene, for a total of four reactions (A−D). Reactions A and C are downhill, whereas reactions B and D are degenerate self-exchange reactions. For all reactions, the OA/RE mechanism was determined as the lowest-energy pathway. Attempts to locate SBM-type pathways for C−H activation in reactions A−D were not successful. Reactions A−D have not been previously studied computationally. Hall reported similar results in his computational studies of the related species $[CpIr(PH_3)Me]^+$ and $[CpIr(PMe_3)Me]^+$ (Cp = η^5-C_5H_5).[24] We repeated Hall's calculations and obtained a similar barrier for methane activation by $[CpIr(PMe_3)Me]^+$.[30] For the complex $[CpIr(PH_3)Me]^+$, Hall found that C−H bond activation was preceded by formation of a methane σ complex.[24a] Our calculations for reactions A−D determined that neither σ-methane complexes nor η^2-benzene π complexes were part of the reaction coordinates.

The calculated activation energies for reactions A−D are 17.30, 21.04, 26.73, and 31.78 kcal/mol (Figure 5). The calculated barriers (A < B < C < D) are consistent with the empirical reaction rates (A > B > C > D). Although the calculated reaction barriers are comprised of both steric and electronic components, the IR ν_{CO} data suggest that the decreased reactivity of the NHC complexes results from steric factors. A comparison of the transition state (TS) structures for

Chart 4. Reactions Studied by DFT

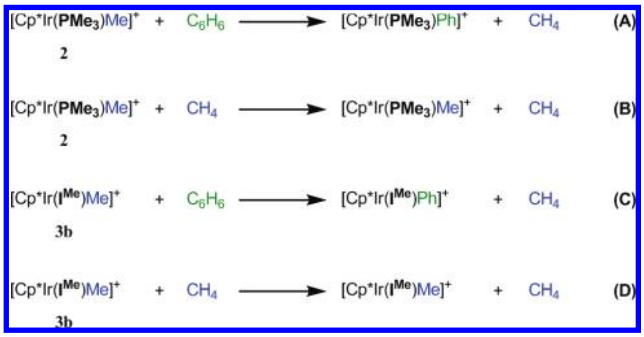

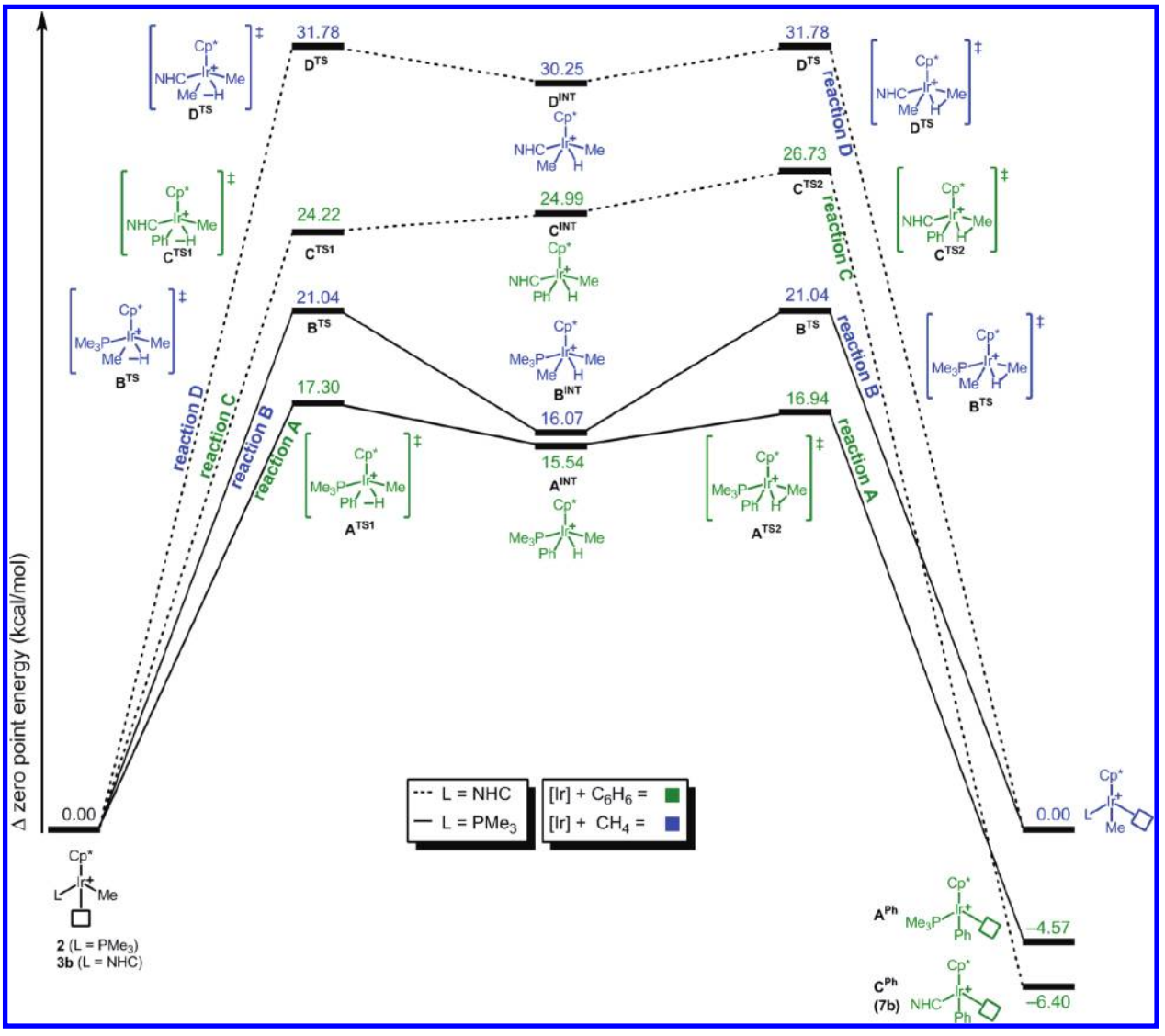

Figure 5. Computational results for reactions A−D. Zero-point energies are given in kcal/mol.

dx.doi.org/10.1021/om2012166 | *Organometallics* 2012, 31, 1879−1887

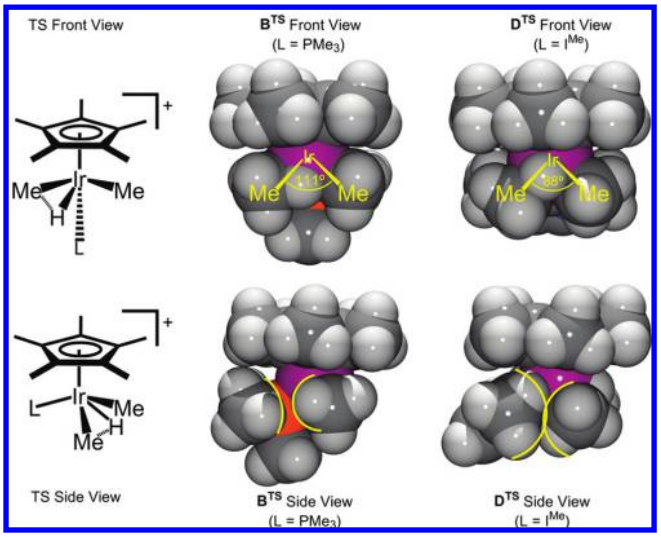

Figure 6. Space-filling models of methane activation TS structures for L = PMe_3 ($\mathbf{B}^{TS}$, left) and L = I^{Me} ($\mathbf{D}^{TS}$, right).

methane activation (reactions B and D) illustrates the differences in steric crowding between **2** and **3b** (Figure 6). The TS structure of the NHC complex ($\mathbf{D}^{TS}$) are more crowded than the phosphine TS structure ($\mathbf{B}^{TS}$). The Me−Ir−Me angles of $\mathbf{B}^{TS}$ and $\mathbf{D}^{TS}$ are 111.09 and 88.34°, respectively.[31] For comparison, the isolable Ir^V species Cp^*IrMe_4, which does not have significant steric crowding, has Me−Ir−Me angles of 113.01° (for transoid Ir−Me groups). Therefore, the large Me−Ir−Me angle in the phosphine TS structure is made possible by the low steric demand of the PMe_3 ligand. A steric clash between the NHC N−Me groups and the Ir−Me groups seems to constrain the Me−Ir−Me angle (Figure 6, right). The calculated HOMOs and LUMOs for $\mathbf{B}^{TS}$ and $\mathbf{D}^{TS}$ are similar and support the assertion that the difference in reactivity is a steric effect.[32]

CONCLUSIONS

A combination of experimental and computational studies were used to examine the C−H bond activation chemistry of the new complexes $[Cp^*Ir(NHC)Me(solv)]^+[MeB(C_6F_5)_3]^-$ (solv = CH_2Cl_2 or open site; **3a−c**). The observed C−H bond activation rates of **3a−c** were significantly slower than similar reactions of the analogous phosphine complex **2**·CH_2Cl_2. DFT calculations confirm that C−H bond activation by **3a−c** is much less kinetically favorable. The calculated structures for Cp*Ir(NHC)-based complexes are more sterically crowded than their phosphine counterparts. Since the NHC-ligated complexes are more electron-rich, it appears that the increased steric demand of the NHC ligands is responsible for the decrease in reactivity. NHC ligands are often used as replacements for phosphine ligands. In the reactions reported here, the increased sterics of the NHC ligands significantly alter the reactivity of the complexes.

EXPERIMENTAL SECTION

General Procedures. Unless otherwise noted, all reactions and manipulations were carried out under an argon atmosphere, using standard Schlenk or glovebox techniques. Oxygen and water were removed from argon prior to use by passage through columns of copper(II) oxide catalyst R3-11 (Chemical Dynamics Corp.) and calcium sulfate (W.A. Hammond Drierite Co.). An MBraun Labmaster 130 glovebox equipped with a Dri-train inert-atmosphere purification system was employed in the manipulation of air-sensitive compounds.

Analytical Techniques. ^1H, ^{11}B, and ^{13}C NMR spectra were acquired using Bruker Avance AV and Avance DRX series 500 MHz spectrometers. A Bruker AV series 300 MHz spectrometer was used to record ^{19}F NMR spectra. Infrared spectra were recorded on a Bruker Tensor 27 spectrometer. EI-MS data were acquired using a Kratos Profile HV-3 direct probe mass spectrometer. Elemental analyses were performed by Atlantic Microlab, Inc., Norcross, GA. ^1H and ^{13}C NMR chemical shifts were referenced to solvent signals and are reported relative to tetramethylsilane as 0 ppm. Chemical shifts in ^{11}B NMR spectra were referenced externally to $BF_3{\cdot}Et_2O$ as 0 ppm. Chemical shifts in ^{19}F NMR spectra were referenced externally to neat CF_3COOH (−76.55 ppm) and are reported relative to $CFCl_3$ as 0 ppm.

Materials. Dichloromethane-d_2 was obtained from Cambridge Isotope Laboratories and vacuum-transferred from calcium hydride prior to use. Benzene was distilled from sodium/potassium/benzophenone ketyl before use. Dichloromethane was dried over activated silica, distilled onto calcium hydride, and distilled again prior to use. Alkanes were treated with sulfuric acid and then dried sequentially with calcium hydride followed by sodium/potassium alloy and distilled prior to use. All other commercially supplied chemicals were used as received. $Cp^*Ir(MeI^{Me})Cl_2$[33] and $B(C_6F_5)_3$[34] were synthesized by reported procedures.

Computational Details. All calculations were carried out in the gas phase using the Gaussian 09 computer program[35] with the B3LYP density functional.[36] The Stuttgart−Dresden (SDD) basis set[37] was employed for the Ir atom with an added d-diffuse (α = 0.05) function. The 631G(d) basis set was used for all non-hydrogen atoms (C, N, and P) and 6-31G(d,p) for the H atoms.[38] All geometries were optimized without symmetry constraints, and zero-point energies (ZPE) were corrected at 298.15 K and 1 atm. Optimized geometries were verified from analytical frequency calculations to give no imaginary frequencies for minima and single imaginary frequencies for the transition states. Examination of the imaginary frequencies with GaussView[39] showed these to be consistent with the corresponding vibrational modes. For $\mathbf{B}^{INT}$, an imaginary frequency from a low-energy oscillation was observed (±0.06 kcal/mol).

$Cp^*Ir(I^{Me})Me_2$ (4b). A Schlenk flask was charged with a stir bar and $Cp^*Ir(I^{Me})Cl_2$ (635 mg, 1.28 mmol).[7] THF (50 mL) was added by static vacuum transfer to produce an orange suspension. While the mixture was stirred vigorously, MeMgBr was added via syringe (2.5 M in diethyl ether, 3.45 mL, 8.63 mmol, 6.7 equiv). The reaction mixture was stirred for 1 h, during which time the orange solids dissolved, resulting in a clear, yellow-brown solution. The volatile materials were removed under reduced pressure to afford an off-white sticky solid. Pentane (70 mL) was added via cannula, and the flask was immersed in a water bath (10 °C). Deionized water (12 mL) was added by syringe over the course of 20 min with stirring. Copious bubbling was observed during the addition of water. The bubbling subsided gradually as the sticky solids were broken apart and dissolved. The yellow supernatant was decanted, via filter cannula, through a glass frit packed with $MgSO_4$ and Celite. The emulsified, brown residue in the reaction flask was extracted with pentane (2 × 50 mL), and the pentane extracts were filtered as above. The pentane extracts were combined, and the volatile materials were removed under reduced pressure to afford **4b** as a pale yellow powder (420 mg, 0.93 mmol, 72%). The crude product was purified by vapor diffusion recrystallization from dichloromethane at −25 °C and/or sublimation (10 mmHg, 140 °C). ^1H NMR (500 MHz, CD_2Cl_2, 25 °C): δ 6.80 (s, 2 H, NHC C−H), 3.56 (s, 6 H, NHC N−Me), 1.63 (s, 15 H, Cp*), −0.05 (s, 6 H, Ir−Me). $^{13}C\{^1H\}$ NMR (126 MHz, CD_2Cl_2, 25 °C): δ 165.96 (s, NHC $C_{carbene}$), 121.12 (s, NHC C−H), 87.67 (s, C_5Me_5), 37.37 (s, NHC N−Me), 8.92 (s, C_5Me_5), −21.04 (s, Ir−Me). Anal. Found (calcd): C, 44.96 (45.01); H, 6.52 (6.44); N, 6.45 (6.18). EI-MS: m/z 454 (M^+), 439 (M^+ − Me).

$Cp^*Ir(MeI^{Me})Me_2$ (4a). The procedure given above for the preparation of **4b** was repeated, using $Cp^*Ir(MeI^{Me})Cl_2$ as the iridium starting material.[7] The crude product was isolated in 71% yield and was purified by recrystallization and/or sublimation. Recrystallization was performed by layering a concentrated dichloromethane solution of crude **4a** with an equal volume of pentane, followed by storage at −10 °C. Typical yields for recrystallization were ca. 50% as yellow

dx.doi.org/10.1021/om2012166 | Organometallics 2012, 31, 1879−1887

rhombus-shaped plates. Sublimation was performed at 10 mmHg and 115 °C. ^{1}H NMR (500 MHz, CD_2Cl_2, 25 °C): δ 3.47 (s, 6 H, NHC N−Me), 2.09 (s, 6 H, NHC C−Me), 1.62 (s, 15 H, Cp*), −0.08 (s, 6 H, Ir−Me). $^{13}C\{^1H\}$ NMR (126 MHz, CD_2Cl_2, 25 °C): δ 163.91 (s, NHC $C_{carbene}$), 123.74 (s, NHC C−Me), 87.34 (s, C_5Me_5), 34.61 (s, NHC N−Me), 10.09 (NHC C−*Me*), 8.88 (s, C_5Me_5), −20.51 (s, Ir−Me). Anal. Found (calcd): C, 47.36 (47.37); H, 6.95 (6.91); N, 5.93 (5.82). EI-MS: *m*/*z* 482 (M^+), 467 (M^+ − Me).

Cp*Ir(BI^{Me})Me$_2$ (4c). The procedure given above for the preparation of **4b** was repeated, using Cp*Ir(BI^{Me})Cl$_2$ as the iridium starting material.[7] The crude product was purified by sublimation (15 mmHg, 125 °C) and isolated in 60% overall yield (120 mg). ^{1}H NMR (500 MHz, CD_2Cl_2, 25 °C): δ 7.24−7.20 (m, 2 H, NHC H_β), 7.17−7.13 (m, 2 H, NHC H_α), 3.76 (s, 6 H, NHC N−Me), 1.68 (s, 15 H, Cp*), 0.03 (s, 6 H, Ir−Me). $^{13}C\{^1H\}$ NMR (126 MHz, CD_2Cl_2, 25 °C): δ 181.88 (s, NHC $C_{carbene}$), 136.56 (s, NHC $C_{bridgehead}$), 121.99 (s, NHC C_α), 109.18 (s, NHC C_β), 88.98 (s, C_5Me_5), 34.21 (s, NHC N−Me), 8.95 (s, C_5Me_5), −19.94 (s, Ir−Me). Anal. Found (calcd): C, 50.25 (50.07); H, 6.19 (6.20); N, 5.44 (5.56). EI-MS: *m*/*z* 504 (M^+), 489 (M^+ − Me).

Cp*Ir(BI^{Me})(CD$_3$)$_2$ (4c-*d*$_6$). On the benchtop, a 50 mL Schlenk flask was charged with Cp*Ir(BI^{Me})Cl$_2$ (131 mg, 240.6 μmol) and a stir bar and then capped with a rubber septum. Diethyl ether was added by static vacuum transfer to produce an orange suspension. While the mixture was stirred vigorously, MeMgI-d_3 was added via syringe (1.0 M in diethyl ether, 2.4 mL, 2.4 mmol, 10 equiv). A colorless precipitate formed immediately upon addition of the Grignard reagent. The reaction mixture was stirred for 1 h, during which time the orange solids dissolved, resulting in a yellow solution with a colorless precipitate. The volatile materials were removed under reduced pressure to afford a yellow oil. Pentane (35 mL) was added via cannula, and the flask was immersed in a water bath (10 °C). Deionized water (1.0 mL) was added by syringe, in three portions, over 10 min with stirring. Copious bubbling was observed during the initial water addition. The yellow supernatant was decanted, via filter cannula, through a glass frit packed with $MgSO_4$ and Celite. The emulsified, pale yellow residue in the reaction flask was extracted with pentane (15 mL), and the pentane extract was filtered as above. The volatile materials were removed from the combined pentane extracts under reduced pressure to afford **4c-*d*$_6$** as a yellow powder (112.3 mg, 220.3 μmol, 92% yield, ca. 95% pure). The crude product was purified by sublimation (10 mmHg, 130 °C), in 84% yield. ^{1}H NMR (500 MHz, CD_2Cl_2, 25 °C): δ 7.24−7.20 (m, 2 H, NHC H_β), 7.17−7.13 (m, 2 H, NHC H_α), 3.76 (s, 6 H, NHC N−Me), 1.68 (s, 15 H, Cp*). ^{2}H NMR (77 MHz, CD_2Cl_2, 25 °C): −0.03 (s, Ir−CD_3).

Characterization of the [MeB(C$_6$F$_5$)$_3$]$^-$ Counteranion in Complexes 3, 7, and 8 by NMR Spectroscopy. ^{1}H NMR (500 MHz, CD_2Cl_2, 25 °C): δ 0.46 (br s, 3 H, fwhh = 10 Hz, B−Me). ^{11}B NMR (160 MHz, CD_2Cl_2, 25 °C): δ −16.01 (s, fwhh =31 Hz). $^{13}C\{^1H\}$ NMR (126 MHz, CD_2Cl_2, 25 °C): δ 148.8 (br d, J_{CF} = 235 Hz, C−F), 138.1 (br d, J_{CF} = 243 Hz, C−F), 137.0 (br d, J_{CF} = 244 Hz, C−F), 129.4 (br s, B−C_{ipso}), B−Me not observed. ^{19}F NMR (282 MHz, CD_2Cl_2, 25 °C): δ −131.93 (br d, J_{FF} = 20 Hz, 6 F, ortho F), −163.98 (t, J_{FF} = 20 Hz, 3 F, para F), −166.60 (m, 6 F, meta F).

[Cp*Ir(I^{Me})Me(solv)]$^+$[MeB(C$_6$F$_5$)$_3$]$^-$ (3b). Solutions of **3b** were prepared *in situ* by the following procedure. In the glovebox, a J. Young NMR tube was charged with Cp*Ir(I^{Me})Me$_2$ (11.3 mg, 24.9 μmol) and B(C$_6$F$_5$)$_3$ (13.6 mg, 26.6 μmol, 1.07 equiv). Dichloromethane-d_2 was added by static vacuum transfer to afford a dark brown solution. ^{1}H NMR (500 MHz, CD_2Cl_2, 25 °C): δ 7.06 (s, 2 H, NHC C−H), 3.49 (s, 6 H, NHC N−Me), 2.36 (s, 3 H, Ir−Me), 1.56 (s, 15 H, Cp*). $^{13}C\{^1H\}$ NMR (126 MHz, CD_2Cl_2, 25 °C): δ 177.16 (s, NHC $C_{carbene}$), 124.41 (s, NHC C−H), 94.99 (s, C_5Me_5), 37.80 (s, NHC N−Me), 20.83 (s, Ir−Me), 10.78 (s, C_5Me_5).

[Cp*Ir(MeI^{Me})Me(solv)]$^+$[MeB(C$_6$F$_5$)$_3$]$^-$ (3a). The procedure given above for **3b** was repeated using **4a** in place of **4b**. ^{1}H NMR (500 MHz, CD_2Cl_2, 25 °C): δ 3.34 (s, 6 H, NHC N−Me), 2.37 (s, 3 H, Ir−Me), 2.21 (s, 6 H, NHC C−Me), 1.55 (s, 15 H, Cp*). $^{13}C\{^1H\}$ NMR (126 MHz, CD_2Cl_2, 25 °C): δ 173.42 (s, NHC $C_{carbene}$), 127.75 (s, NHC C−Me), 94.60 (s, C_5Me_5), 35.19 (s, NHC N−Me), 20.89 (s, Ir−Me), 10.79 (s, C_5Me_5), 9.14 (s, NHC C−*Me*).

[Cp*Ir(BI^{Me})Me(solv)]$^+$[MeB(C$_6$F$_5$)$_3$]$^-$ (3c). The procedure given above for **3b** was repeated using **4c** in place of **4b**. ^{1}H NMR (500 MHz, CD_2Cl_2, 25 °C): δ 7.50−7.46 (m, 2 H, NHC H_β), 7.45−7.41 (m, 2 H, NHC H_α), 3.70 (s, 6 H, NHC N−Me), 2.41 (s, 3 H, Ir−Me), 1.68 (s, 15 H, Cp*). $^{13}C\{^1H\}$ NMR (126 MHz, CD_2Cl_2, 25 °C): δ 187.90 (s, NHC $C_{carbene}$), 136.09 (s, NHC $C_{bridgehead}$), 124.68 (s, NHC C_α), 110.96 (s, NHC C_β), 95.95 (s, C_5Me_5), 34.84 (s, NHC N−Me), 19.3 (Ir−Me), 10.87 (s, C_5Me_5).

[Cp*Ir(BI^{Me})CD$_3$(solv)]$^+$[(CD$_3$)B(C$_6$F$_5$)$_3$]$^-$ (3c-*d*$_6$). The procedure above was repeated using **4c-*d*$_6$**. ^{1}H NMR (500 MHz, CD_2Cl_2, 25 °C): δ 7.50−7.46 (m, 2 H, NHC H_β), 7.45−7.41 (m, 2 H, NHC H_α), 3.70 (s, 6 H, NHC N−Me), 1.60 (s, 15 H, Cp*). ^{2}H NMR (77 MHz, CD_2Cl_2, 25 °C) δ 2.40 (s, fwhh = 0.7 Hz, 3 D, Ir−CD_3), 0.46 (br s, fwhh =3.8 Hz, 3 D, B−CD_3). ^{11}B NMR (160 MHz, CD_2Cl_2, 25 °C): δ −15.87 (s, fwhh = 31 Hz). $^{13}C\{^1H\}$ NMR (126 MHz, CD_2Cl_2, 25 °C): δ 187.88 (s, NHC $C_{carbene}$), 148.8 (br d, J_{CF} = 235 Hz, ([(CD$_3$)B(C$_6$F$_5$)$_3$]$^-$, C−F), 138.0 (br m, J_{CF} = 243 Hz, ([(CD$_3$)B(C$_6$F$_5$)$_3$]$^-$, C−F), 136.9 (br ddd, J_{CF} = 245, 23, 12 Hz, [(CD$_3$)B(C$_6$F$_5$)$_3$]$^-$, C−F), 136.07 (s, NHC $C_{bridgehead}$), 129.5 (v br s, [(CD$_3$)B(C$_6$F$_5$)$_3$]$^-$, C ipso), 124.66 (s, NHC C_α), 110.94 (s, NHC C_β), 95.92 (s, C_5Me_5), 34.82 (s, NHC N−Me), 19.27 (5 lines observed, septet expected, J_{CD} = 19.6 Hz, Ir−CD_3), 10.85 (s, C_5Me_5), B−CD_3 not observed.

[Cp*Ir(I^{Me})Me(CO)]$^+$[MeB(C$_6$F$_5$)$_3$]$^-$ (5b). In the glovebox, a 75 mL pressure flask equipped with a resealable Teflon valve was charged with a stir bar, Cp*Ir(I^{Me})Me$_2$ (29.4 mg, 64.7 μmol), and B(C$_6$F$_5$)$_3$ (35.1 mg, 68.6 μmol, 1.06 equiv). Dichloromethane was added by static vacuum transfer (5 mL), and the mixture was pressurized with CO (0.1 atm, dried over 4 Å molecular sieves) at −78 °C. The solution was warmed to ambient temperature over 30 min while stirring. The color changed from dark brown to faint yellow. Stirring was continued for an additional 4 h, at which point the flask was backfilled with argon and pentane was added by cannula (50 mL). Stirring caused precipitation of **5b** as a light pink oil. The supernatant was decanted, and the volatile materials were removed to afford 56 mg of **5b** (87% yield). ^{1}H NMR (500 MHz, CD_2Cl_2, −33 °C): δ 7.14 (d, J_{HH} = 1.7 Hz, 1 H, NHC C−H), 7.05 (d, J_{HH} = 1.7 Hz, 1 H, NHC C−H), 3.70 (s, 3 H, NHC N−Me), 3.51 (s, 3 H, NHC N−Me), 1.90 (s, 15 H, Cp*), 0.71 (s, 3 H, Ir−Me), 0.39 (br s, 3 H, B−Me). ^{1}H NMR (500 MHz, CD_2Cl_2, 25 °C): δ 7.11 (br s, 2 H, NHC C−H), 3.65 (br s, 6 H, NHC N−Me), 1.94 (s, 15 H, Cp*), 0.78 (s, 3 H, Ir−Me), 0.46, (br s, 3 H, B−Me). ^{11}B NMR (160 MHz, CD_2Cl_2, 25 °C): δ −16.01 (s, fwhh = 30 Hz). $^{13}C\{^1H\}$ NMR (126 MHz, CD_2Cl_2, 25 °C): δ 168.99 (s, NHC $C_{carbene}$), 140.33 (s, Ir−CO), 124.98 (s, NHC C−H), 100.56 (C_5Me_5), 39.6 (br s, NHC N−Me), 9.31 (s, C_5Me_5), −26.10 (s, Ir−Me). ^{19}F NMR (471 MHz, CD_2Cl_2, 25 °C): δ −131.92 (br d, J_{FF} = 20 Hz, 6 F, [MeB(C$_6$F$_5$)$_3$]$^-$ ortho F), −163.95 (t, J_{FF} = 20 Hz, 3 F, [MeB(C$_6$F$_5$)$_3$]$^-$ para F),−166.56 (br m, 6 F, [MeB(C$_6$F$_5$)$_3$]$^-$ meta F). IR (CH_2Cl_2): ν_{CO} 2024 cm^{-1}. Anal. Found (calcd): C, 43.44 (43.52); H, 2.83 (2.94); N, 2.86 (2.82); F, 28.88 (28.68).

Crystals of [{Cp*Ir(I^{Me})(μ-Cl)}$_2$]$^{2+}$ (6b) Used for X-ray Diffraction. A dichloromethane-d_2 solution of **3b** (32.4 μmol) was prepared in a J. Young NMR tube as described above. After 5 days, crystals of **6b** had deposited (ca. 6 mg, 3 μmol, 10% yield).

[Cp*Ir(I^{Me})Ph(solv)]$^+$[MeB(C$_6$F$_5$)$_3$]$^-$ (7b). A solution of **3b** (47.8 μmol) in CD_2Cl_2 was prepared in a J. Young NMR tube as described above. Benzene (0.467 g, 5.97 mmol, 125 equiv) was added to this solution by static vacuum transfer. After 24 h, the volatile components were removed under reduced pressure to afford an oily, dark reddish-brown residue. After CD_2Cl_2 was added to this material by static vacuum transfer and shaking, a homogeneous dark brown solution resulted (90% NMR yield). ^{1}H NMR (500 MHz, CD_2Cl_2, 25 °C): δ 7.36 (s, free C_6H_6, 1.3 equiv), 7.30−7.15 (m, 5 H, Ir−Ph), 7.13 (s, 2 H, NHC C−H), 3.54 (s, 6 H, NHC N−Me), 1.65 (s, 15 H, Cp*). $^{13}C\{^1H\}$ NMR (126 MHz, CD_2Cl_2, 25 °C): δ 175.64 (s, NHC $C_{carbene}$), 165.18 (s, Ir−Ph ipso), 138.87 (s, Ir−Ph), 129.73 (s, Ir−Ph), 128.94 (s, Ir−Ph) 128.88 (s, free C_6H_6), 124.70 (s, NHC C−H), 96.22 (s, C_5Me_5), 38.59 (s, NHC N−Me), 11.12 (s, C_5Me_5).

dx.doi.org/10.1021/om2012166 | *Organometallics* 2012, 31, 1879−1887

[Cp*Ir(MeI^{Me})Ph(solv)]$^+$[MeB(C$_6$F$_5$)$_3$]$^-$ (7a). This compound was prepared as above for **7b**. ^{1}H NMR (500 MHz, CD_2Cl_2, 25 °C): δ 7.36 (s, free C_6H_6, 2 equiv), 7.26−7.14 (m, 5 H, Ir−Ph), 3.39 (s, 6 H, NHC N−Me), 2.24 (s, 6 H, NHC C−Me), 1.64 (s, 15 H, Cp*). ^{13}C{^{1}H} NMR (126 MHz, CD_2Cl_2, 25 °C): δ 171.90 (s, NHC $C_{carbene}$), 165.48 (s, Ir−Ph ipso), 138.57 (s, Ir−Ph ortho), 129.32 (s, Ir−Ph para), 128.89 (s, free C_6H_6) 128.86 (s, Ir−Ph meta), 128.17 (s, NHC *C*−Me), 95.92 (s, C_5Me_5), 36.05 (s, NHC N−Me), 11.12 (s, C_5Me_5), 9.30 (s, NHC C−*Me*).

[Cp*Ir(MeI^{Me})(C$_6$H$_4$F)(solv)]$^+$[MeB(C$_6$F$_5$)$_3$]$^-$ (8a). In the glovebox, a J. Young NMR tube was charged with Cp*Ir(MeI^{Me})Me$_2$ (8.8 mg, 18.3 μmol) and B(C$_6$F$_5$)$_3$ (9.3 mg, 18.2 μmol, 0.99 equiv). Fluorobenzene (0.432 g, 0.43 mL, 250 equiv) was added by static vacuum transfer. Monitoring the resulting dark brown solution by NMR spectroscopy showed that the reaction was 33% complete after 1 day, 72% complete after 2 days, and 100% complete after 3 days. The volatiles were removed under reduced pressure. Dichloromethane-d_2 was added by static vacuum transfer to afford a red-brown homogeneous solution. ^{1}H NMR (500 MHz, CD_2Cl_2, 25 °C): free C_6H_5F, δ 7.36, 7.16, 7.06; δ for isomeric mixture of **8a** (integrations are internally consistent for each isomer and do not reflect the ratio of products; many of the Ir−Ph signals are overlapping), 7.26 (m, 1 H, Ir(*m*-PhF) meta H), 7.18 (m, 2 H, Ir(*p*-PhF) meta H), 7.08 (m, 2H, Ir(*o*-PhF) meta H), 6.99 (m, 1 H, Ir(*o*-PhF) para H), 6.94 (m, 1 H, Ir(*o*-PhF) ortho H), 6.93 (m, 2 H, Ir(*p*-PhF) ortho H), 6.91 (m, 1 H, Ir(*m*-PhF) para H), 6.83 (v tdd, J_{HH} = 9.0 Hz, J_{HF} = 2.7 Hz, J_{HH} = 0.8 Hz, 1 H, Ir(*m*-PhF) ortho H), 6.77 (ddd, J_{HF} = 9.5 Hz, J_{HH} = 2.5, 0.8 Hz, 1 H, Ir(*m*-PhF) ortho H), 3.39 (2 × s (overlapping), 2 × 6 H, Ir(*o*-PhF) NHC N−Me and Ir(*m*-PhF) NHC N−Me), 3.37 (s, 6 H, Ir(*p*-PhF)NHC N−Me), 2.24 (s, 6 H, Ir(*p*-PhF) NHC C−Me), 2.23 (s, 6 H, Ir(*m*-PhF) NHC C−Me), 2.17 (s, 6 H, Ir(*o*-PhF) NHC C−Me), 1.64 (s, 15 H, Ir(*p*-PhF) Cp*), 1.62 (s, 15 H, Ir(*m*-PhF) Cp*), 1.57 (s, 15 H, Ir(*o*-PhF) Cp*), 0.46 (br s, 3 H, B−Me). ^{13}C{^{1}H} NMR (126 MHz, CD_2Cl_2, 25 °C): δ 176.26 (s, NHC $C_{carbene}$), 170.36 (s, NHC $C_{carbene}$), 134.79, 134.66, 132.44, 130.04, 129.98, 129.62, 129.57, 127.83 (s, Ir(*m*-PhF) NHC *C*−Me), 127.74 (s, Ir(*p*-PhF) NHC *C*−Me), 127.71 (s, Ir(*o*-PhF) NHC *C*−Me), 124.72, 124.08, 124.06, 122.94, 122.81, 115.24, 115.19, 115.08, 114.78, 114.55, 114.49, 114.32, 95.65 (s, Ir(*m*-PhF) C_5Me_5), 95.44 (s, Ir(*p*-PhF) C_5Me_5), 95.34 (s, Ir(*o*-PhF) C_5Me_5), 35.51 (s, Ir(*p*-PhF) NHC N−Me), 35.38 (s, Ir(*m*-PhF) NHC N−Me), 35.00 (s, Ir(*o*-PhF) NHC N−Me), 10.56 (s, Ir(*p*-PhF) C_5Me_5), 10.48 (s, Ir(*m*-PhF) C_5Me_5), 10.39 (s, Ir(*o*-PhF) C_5Me_5), 10.22 (s, B−Me), 8.72 (s, Ir(*p*-PhF) NHC C−*Me*), 8.68 (s, Ir(*m*-PhF) NHC C−*Me*), 8.53 (s, Ir(*o*-PhF) NHC C−*Me*). ^{19}F NMR (471 MHz, CD_2Cl_2, 25 °C): δ −88.34 (m, Ir(*o*-PhF)), −109.61 (m, Ir(*p*-PhF)), −112.98 (m, free C_6H_5F), −113.785 (m, Ir(*m*-PhF)).

Reaction between [Cp*Ir(BI^{Me})Me(solv)]$^+$[MeB(C$_6$F$_5$)$_3$]$^-$ (3c) and Cyclohexane. Cyclohexane (0.399 g, 4.7 mmol, 220 equiv) was added to a solution of [Cp*Ir(BI^{Me})Me(solv)]$^+$[MeB(C$_6$F$_5$)$_3$]$^-$ (22 μmol) in dichloromethane-d_2 (0.610 g, 7.1 mmol, 330 equiv) by static vacuum transfer. The resulting homogeneous dark brown solution was monitored by NMR spectroscopy over 28 days. During this time a small quantity of methane was evolved. A small quantity of [Cp*Ir(BI^{Me})(H)-(cyclohexene)]$^+$[MeB(C$_6$F$_5$)$_3$]$^-$ was observed by ^{1}H NMR spectroscopy (16%). ^{1}H NMR (500 MHz, CD_2Cl_2/cyclohexane, 25 °C): δ 7.56 (d, J_{HH} = 8.4 Hz, 1 H, NHC Ar H), 7.5 (1 H, NHC Ar H, signal hidden under Ar H of IrMe$^+$), 7.18 (t, J_{HH} = 8.4 Hz, 1 H, NHC Ar−H), 6.40 (d, J_{HH} = 6.4 Hz, 1 H, NHC Ar H), 3.90 (s, 3 H, NHC N−Me), 3.13 (s, 3 H, NHC N−Me), 2.08 (s, 15 H, Cp*), 0.58 (br s, B−Me), −13.84 (s, 1 H, hydride), a singlet was observed at 0.28 ppm and is attributed to methane; signals between 4.4 and 0.9 ppm may be attributed to the Ir−cyclohexene group but were not assigned.

Attempted Reaction of [Cp*Ir(BI^{Me})(CD$_3$)]$^+$[D$_3$CB(C$_6$F$_5$)$_3$]$^-$ (3c-*d*$_6$) with CH$_4$. A dichloromethane-d_2 solution of [Cp*Ir(BI^{Me})CD$_3$]$^+$-[D$_3$CB(C$_6$F$_5$)$_3$]$^-$ (28.1 μmol) was prepared as described above in a medium-walled J.Young NMR tube. The sample was degassed by freeze−pump−thaw cycles and pressurized with CH_4 using a brass gas addition manifold (3 atm, 99.99% pure). No immediate reaction was observed. The sample was stored in the absence of light and monitored periodically by NMR spectroscopy. No incorporation of ^{1}H nuclei into the Ir−Me or B−Me groups was observed by ^{1}H NMR spectroscopy after 120 days. A small amount of CD_3H was observed by ^{2}H NMR spectroscopy; however, the absence of protiated Ir−Me groups suggests that CD_3H was formed by hydrolysis. The ^{11}B and ^{19}F NMR signals were unchanged throughout the course of the reaction.

■ ASSOCIATED CONTENT

Ⓢ Supporting Information

Text, figures, tables, and CIF files giving experimental details regarding the syntheses of Cp*Ir(NHC)Cl$_2$, X-ray crystallographic data for complexes **4a,b**, **6b**, and Cp*Ir(BI^{Me})Cl$_2$, NMR spectra of selected species, including all nonisolated complexes, UV/vis spectrum of **3b**, details of crystallographic data collection, and details of the calculations. This material is available free of charge via the Internet at http://pubs.acs.org.

■ AUTHOR INFORMATION

Corresponding Author

*E-mail: heinekey@chem.washington.edu.

Notes

The authors declare no competing financial interest.

■ ACKNOWLEDGMENTS

This work was supported by the NSF as part of the Center for Enabling New Technologies through Catalysis (CENTC; Grant No. CHE-0650456). We thank Marion H. Emmert, Elon A. Ison, William D. Jones, James M. Mayer, and Melanie S. Sanford for helpful discussions. We thank a reviewer for helpful suggestions regarding DFT calculations.

■ REFERENCES

(1) (a) Labinger, J. A.; Herring, A. M.; Lyon, D. K.; Luinstra, G. A.; Bercaw, J. E.; Horvath, I. T.; Eller, K. *Organometallics* **1993**, *12*, 895−905. (b) Luinstra, G. A.; Wang, L.; Stahl, S. S.; Labinger, J. A.; Bercaw, J. E. *Organometallics* **1994**, *13*, 755−756. (c) Hutson, A. C.; Lin, M.; Basickes, N.; Sen, A. *J. Organomet. Chem.* **1995**, *504*, 69−74. (d) Luinstra, G. A.; Wang, L.; Stahl, S. S.; Labinger, J. A.; Bercaw, J. E. *J. Organomet. Chem.* **1995**, *504*, 75−91. (e) Stahl, S. S.; Labinger, J. A.; Bercaw, J. E. *J. Am. Chem. Soc.* **1996**, *118*, 5961−5976. (f) Holtcamp, M. W.; Labinger, J. A.; Bercaw, J. E. *Inorg. Chim. Acta* **1997**, *265*, 117−125. (g) Holtcamp, M. W.; Henling, L. M.; Day, M. W.; Labinger, J. A.; Bercaw, J. E. *Inorg. Chim. Acta* **1998**, *270*, 467−478. (h) Fekl, U.; Zahl, A.; van Eldik, R. *Organometallics* **1999**, *18*, 4156−4164. (i) Fekl, U.; Kaminsky, W.; Goldberg, K. I. *J. Am. Chem. Soc.* **2001**, *123*, 6423−6424. (j) Scollard, J. D.; Day, M.; Labinger, J. A.; Bercaw, J. E. *Helv. Chim. Acta* **2001**, *84*, 3247−3268. (k) Fekl, U.; Goldberg, K. I. *J. Am. Chem. Soc.* **2002**, *124*, 6804−6805.

(2) Young, K. J. H.; Oxgaard, J.; Ess, D. H.; Meier, S. K.; Stewart, T.; Goddard, W. A. III; Periana, R. A. *Chem. Commun.* **2009**, 3270−3272.

(3) (a) Periana, R. A.; Taube, D. J.; Gamble, S.; Taube, H.; Satoh, T.; Fujii, H. *Science* **1998**, *280*, 560−564. (b) Muehlhofer, M.; Strassner, T.; Herrmann, W. A. *Angew. Chem., Int. Ed.* **2002**, *41*, 1745−1747. (c) Ahrens, S.; Zeller, A.; Taige, M.; Strassner, T. *Organometallics* **2006**, *25*, 5409−5415. (d) Meyer, D.; Taige, M. A.; Zeller, A.; Hohlfeld, K.; Ahrens, S.; Strassner, T. *Organometallics* **2009**, *28*, 2142−2149.

(4) Arndtsen, B. A.; Bergman, R. G. *Science* **1995**, *270*, 1970−1973.

(5) (a) Hanasaka, F.; Tanabe, Y.; Fujita, K.-I.; Yamaguchi, R. *Organometallics* **2006**, *25*, 826−831. (b) Tanabe, Y.; Hanasaka, F.; Fujita, K.-I.; Yamaguchi, R. *Organometallics* **2007**, *26*, 4618−4626. (c) Corberan, R.; Sanau, M.; Peris, E. *Organometallics* **2006**, *25*, 4002−4008.

(6) Gusev, D. G. *Organometallics* **2009**, *28*, 6458−6461.

(7) See the Supporting Information for details regarding the syntheses of Cp*Ir(NHC)Cl$_2$ complexes and characterization of the new complex Cp*Ir(BI^{Me})Cl$_2$.

(8) For the ORTEP of complex **4a**, see the Supporting Information
(9) For the UV/vis spectrum of complex **3b**, see the Supporting Information.
(10) Details regarding the reactions of **3a**−**c** with O_2 will be reported elsewhere.
(11) Silverstein, R. M.; Webster, F. X.; Kiemie, D. *Spectrometric Identification of Organic Compounds*, 7th ed.; Wiley: Chichester, U.K., 2002; p 209.
(12) Brookhart, M.; Green, M. L. H. *J. Organomet. Chem.* **1983**, *250*, 395−408.
(13) (a) Guzei, I. A.; Stockland, R. A. Jr.; Jordan, R. F. *Acta Crystallogr., Sect. C: Cryst. Struct. Commun.* **2000**, *C56*, 635−636. (b) Varga, V.; Pinkas, J.; Cisarova, I.; Horacek, M.; Mach, K. *Organometallics* **2009**, *28*, 6944−6956. (c) Munha, R. F.; Antunes, M. A.; Alves, L. G.; Veiros, L. F.; Fryzuk, M. D.; Martins, A. M. *Organometallics* **2010**, *29*, 3753−3764.
(14) (a) Peters, J. C.; Feldman, J. D.; Tilley, T. D. *J. Am. Chem. Soc.* **1999**, *121*, 9871−9872. (b) Guo, Z.; Swenson, D. C.; Guram, A. S.; Jordan, R. F. *Organometallics* **1994**, *13*, 766−773. (c) Bibal, C.; Santini, C. C.; Chauvin, Y.; Vallee, C.; Olivier-Bourbigou, H. *Dalton Trans.* **2008**, 2866−2870. (d) Munha, R. F.; Antunes, M. A.; Alves, L. G.; Veiros, L. F.; Fryzuk, M. D.; Martins, A. M. *Organometallics* **2010**, *29*, 3753−3764. (e) Sanchez-Nieves, J.; Tabernero, V.; Camejo, C.; Royo, P. *J. Organomet. Chem.* **2010**, *695*, 2469−2473.
(15) (a) Alaimo, P. J.; Arndtsen, B. A.; Bergman, R. G. *J. Am. Chem. Soc.* **1997**, *119*, 5269−5270. (b) Alaimo, P. J.; Arndtsen, B. A.; Bergman, R. G. *Organometallics* **2000**, *19*, 2130−2143. (c) Cartwright, S. A.; White, P.; Brookhart, M. *Organometallics* **2006**, *25*, 1664−1675. (d) Polukeev, A. V.; Kuklin, S. A.; Petrovskii, P. V.; Peregudov, A. S.; Dolgushin, F. M.; Ezernitskaya, M. G.; Koridze, A. A. *Russ. Chem. Bull.* **2010**, *59*, 745−749.
(16) Tellers, D. M.; Skoog, S. J.; Bergman, R. G.; Gunnoe, T. B.; Harman, W. D. *Organometallics* **2000**, *19*, 2428−2432.
(17) Ohki, Y.; Sakamoto, M.; Tatsumi, K. *J. Am. Chem. Soc.* **2008**, *130*, 11610−11611.
(18) Feng, Y.; Jiang, B.; Boyle, P. A.; Ison, E. A. *Organometallics* **2010**, *29*, 2857−2867.
(19) (a) Winter, C. H.; Gladysz, J. A. *J. Organomet. Chem.* **1988**, *354*, C33−C36. (b) Fernandez, J. M.; Gladysz, J. A. *Organometallics* **1989**, *8*, 207−219. (c) Peng, T.-S.; Winter, C. H.; Gladysz, J. A. *Inorg. Chem.* **1994**, *33*, 2534−2542.
(20) Winter, C. H.; Arif, A. M.; Gladysz, J. A. *Organometallics* **1989**, *8*, 219−25.
(21) Samples of **3a**−**c** dissolved in CH_2Cl_2 and exposed to laboratory light under an argon atmosphere decomposed to intractable products in ca. 3 weeks at ambient temperature.
(22) Klei, S. R.; Golden, J. T.; Burger, P.; Bergman, R. G. *J. Mol. Catal. A: Chem.* **2002**, *189*, 79−94.
(23) For more information, see the Supporting Information
(24) (a) Strout, D. L.; Zaric, S.; Niu, S.; Hall, M. B. *J. Am. Chem. Soc.* **1996**, *118*, 6068−6069. (b) Su, M.-D.; Chu, S.-Y. *J. Am. Chem. Soc.* **1997**, *119*, 5373−5383. (c) Niu, S.; Hall, M. B. *J. Am. Chem. Soc.* **1998**, *120*, 6169−6170. (d) Anstey, M. R.; Yung, C. M.; Du, J.; Bergman, R. G. *J. Am. Chem. Soc.* **2007**, *129*, 776−777.
(25) (a) Hinderling, C.; Plattner, D. A.; Chen, P. *Angew. Chem., Int. Ed.* **1997**, *36*, 243−244. (b) Hinderling, C.; Feichtinger, D.; Plattner, D. A.; Chen, P. *J. Am. Chem. Soc.* **1997**, *119*, 10793−10804.
(26) (a) Gilbert, T. M.; Bergman, R. G. *Organometallics* **1983**, *2*, 1458−1460. (b) Gilbert, T. M.; Hollander, F. J.; Bergman, R. G. *J. Am. Chem. Soc.* **1985**, *107*, 3508−3516. (c) Ricci, J. S. Jr.; Koetzle, T. F.; Fernandez, M. J.; Maitlis, P. M.; Green, J. C. *J. Organomet. Chem.* **1986**, *299*, 383−389.
(27) (a) Alaimo, P. J.; Bergman, R. G. *Organometallics* **1999**, *18*, 2707−2717. (b) Klei, S. R.; Tilley, T. D.; Bergman, R. G. *J. Am. Chem. Soc.* **2000**, *122*, 1816−1817. (c) Klei, S. R.; Tilley, T. D.; Bergman, R. G. *Organometallics* **2001**, *20*, 3220−3222. (d) Reference 17.
(28) (a) See ref 26. (b) Kawamura, K.; Hartwig, J. F. *J. Am. Chem. Soc.* **2001**, *123*, 8422−8423. (c) Lee, Y.-J.; Lee, J.-D.; Kim, S.-J.; Ko, J.; Suh, I.-H.; Cheong, M.; Kang, S. O. *Organometallics* **2004**, *23*, 135−143.
(29) Crabtree, R. H. *The Organometallic Chemistry of the Transition Metals*, 4th ed.; Wiley: Hoboken, NJ, 2005; pp 176−177.
(30) Hall reported an activation energy of 13.0 kcal/mol;[24c] we obtained 13.79 kcal/mol.
(31) Angles measured with the computer program Mercury: (a) Taylor, R.; Macrae, C. F. *Acta Crystallogr., Sect. B: Struct. Sci.* **2001**, *B57*, 815−827. (b) Bruno, I. J.; Cole, J. C.; Edgington, P. R.; Kessler, M.; Macrae, C. F.; McCabe, P.; Pearson, J.; Taylor, R. *Acta Crystallogr., Sect. B: Struct. Sci.* **2002**, *B58*, 389−397. (c) Macrae, C. F.; Edgington, P. R.; McCabe, P.; Pidcock, E.; Shields, G. P.; Taylor, R.; Towler, M.; van, d. S. J. *J. Appl. Crystallogr.* **2006**, *39*, 453−457. (d) Macrae, C. F.; Bruno, I. J.; Chisholm, J. A.; Edgington, P. R.; McCabe, P.; Pidcock, E.; Rodriguez-Monge, L.; Taylor, R.; van, d. S. J.; Wood, P. A. *J. Appl. Crystallogr.* **2008**, *41*, 466−470.
(32) For graphical depictions of the HOMO and LUMO for all calculated structures, see the Supporting Information.
(33) Hanasaka, F.; Fujita, K.-i.; Yamaguchi, R. *Organometallics* **2004**, *23*, 1490−1492.
(34) (a) Massey, A. G.; Park, A. J.; Stone, F. G. A. *Proc. Chem. Soc., London* **1963**, 212. (b) Massey, A. G.; Park, A. J. *J. Organomet. Chem.* **1964**, *2*, 245−520. (c) Pohlmann, J. L. W.; Brinckman, F. E. *Z. Naturforsch.* **1965**, *20b*, 5−11. (d) Massey, A. G.; Park, A. J. *J. Organomet. Chem.* **1966**, *5*, 218−225.
(35) For the full Gaussian 09 reference, see the Supporting Information.
(36) (a) Becke, A. D. *J. Chem. Phys.* **1993**, *98*, 5648. (b) Lee, C.; Yang, W.; Parr, R. G. *Phys. Rev. B* **1988**, *37*, 785. (c) Stephens, P. J.; Devlin, F. J.; Chabalowski, C. F.; Frish, M. J. *J. Phys. Chem.* **1994**, *98*, 11623.
(37) Andrae, D.; Häußermann, U.; Dolg, M.; Stoll, H.; Preuß, H. *Theor. Chem. Acc.* **1990**, *77*, 123.
(38) (a) Hariharan, P. C.; Pople, J. A. *Theor. Chim. Acta* **1973**, *28*, 213−222. (b) Petersson, G. A.; Al-Laham, M. A. *J. Chem. Phys.* **1991**, *94*, 6081−6090. (c) Petersson, G. A.; Bennett, A.; Tensfeldt, T. G.; Al-Laham, M. A.; Shirley, W. A.; Mantzaris, J. *J. Chem. Phys.* **1988**, *89*, 2193−2218.
(39) *GaussView 5.0*; Gaussian, Inc., 2008.